KFA-IKP(Th)-1996-11
TK 96 26
nucl-th/9609051

Threshold kaon photo- and electroproduction in SU(3) baryon chiral perturbation theory

S. Steininger[†#1], Ulf-G. Meißner[‡#2]

[†]Universität Bonn, Institut für Theoretische Kernphysik
Nussallee 14-16, D-53115 Bonn, Germany

[‡]Forschungszentrum Jülich, Institut für Kernphysik (Theorie)
D-52425 Jülich, Germany

Abstract

We calculate the processes $\gamma p \to K^0\Sigma^+, K^+\Sigma^0, K^+\Lambda$ in three flavor heavy baryon chiral perturbation theory to one loop. Some low–energy constants are fixed from single baryon properties while others are estimated by means of resonance saturation. The total cross sections are comparable with the few existing data points in the threshold region. The angular dependences of the recoil polarization of the Λ and Σ^0 show most features of the ones measured at ELSA. We also predict the isovector charge radius of the Σ^+, $\langle r_V^2\rangle_{\Sigma^+} = (0.30 \pm 0.03)\,\mathrm{fm}^2$.

[#1]email: sven@pythia.itkp.uni-bonn.de
[#2]email: Ulf-G.Meissner@kfa-juelich.de

1. Threshold pion photo- and electroproduction has been at the center of numerous experimental studies at MAMI, SAL and NIKHEF over the last few years. These data serve as one of the major testing grounds of baryon chiral perturbation theory which allows to sharpen our understanding of the spontaneous and explicit chiral symmetry breaking in QCD. One particularly spectacular example is the process $\gamma p \to \pi^0 p$ which clearly shows the relevance of chiral (pion) loops in the electric dipole amplitude and has also lead to novel low–energy theorems related to some of the P–wave multipoles [1][2]. With the emergence of kaon photoproduction data from ELSA at Bonn (total and differential cross sections as well as hyperon recoil polarizations) [3][4], it appears natural to extend the successful SU(2) pion production calculations to the three–flavor case.[#3] Evidently, while for SU(2) the pertinent expansion parameter is small, $M_\pi/4\pi F_\pi = 0.12$ (with M_π and F_π the pion mass and decay constant, respectively), the larger strange quark mass leads to $M_K/4\pi F_\pi = 0.43$ (with M_K the kaon mass). Therefore, it is a priori not clear whether the method of expanding S–matrix elements and transition currents in small momenta and meson masses, which is at the heart of chiral perturbation theory (CHPT), is applicable in the presence of baryons. In this letter, we show the results of such an exploratory study which lends some credit to the usefulness of the method.

2. The starting point of the heavy baryon CHPT [5][6] is an effective Lagrangian formulated in terms of the asymptotic fields, here the octet of Goldstone bosons (collected in the matrix–valued field $U(x)$) and the ground state baryon octet, denoted B. It admits a low energy expansion of the form

$$\mathcal{L}_{\rm eff} = \mathcal{L}_M + \mathcal{L}_{MB} = \mathcal{L}_M^{(2)} + \mathcal{L}_{MB}^{(1)} + \mathcal{L}_{MB}^{(2)} + \mathcal{L}_{MB}^{(3)} + \ldots \tag{1}$$

where the subscript $'M'$ ($'MB'$) denotes the meson (meson–baryon) sector and the superscript $'(i)'$ the chiral dimension. The ellipsis stands for terms of higher order not needed here. Beyond leading order, the effective Lagrangian contains parameters not fixed by chiral symmetry, the so–called low–energy constants. In principle, these LECs should be pinned down from data or calculated by means of lattice gauge theory. To some extent, their values reflect the spectrum of QCD [7] which has lead to the resonance exchange saturation hypothesis. This somewhat model–dependent method to estimate the LECs is an indispensible tool in the absence of a sufficiently complete body of accurate data. The form of $\mathcal{L}_{MB}^{(1)}$ is standard, we use here the notation of ref.[8], and from $\mathcal{L}_{MB}^{(2)}$ we only need the magnetic photon baryon (transition) couplings. At third order in the energy expansion, we have in total 15 terms contributing to the S– and P–waves,

$$\mathcal{L}_{MB}^{(3)} = \sum_{i=1}^{13} d_i\, O_i + d_{14}\, O_{14} + d_{15}\, O_{15} \ , \tag{2}$$

with the last two terms related to baryon octet isovector charge radii and only of relevance for electroproduction. The LECs d_1 and d_2 enter the axial (transition) radii and one combination can be fixed from the nucleon axial radius (see below). We work to order q^3

[#3] The data of ref.[4] are not yet available.

in the small momentum expansion, i.e. we have to consider tree graphs with insertions from $\mathcal{L}_{MB}^{(1,2,3)}$ and one loop diagrams with insertions from $\mathcal{L}_{MB}^{(1)}$.

3. Consider now the reactions $\gamma(k)+p(p_1)\to K^0(q)+\Sigma^+(p_2)\,,\ K^+(q)+\Sigma^0(p_2)\,,\ K^+(q)+\Lambda(p_2)$, with γ a real ($k^2=0$) or a virtual ($k^2<0$) photon. In the threshold region, the transition matrix–element can be written in terms of S– and P–wave multipoles (for photoproduction),

$$\frac{m}{4\pi\sqrt{s}}T\cdot\varepsilon = i\vec{\sigma}\cdot\vec{\varepsilon}(E_{0+}+\hat{k}\cdot\hat{q}\,P_1)+i\vec{\sigma}\cdot\hat{k}\,\vec{\varepsilon}\cdot\hat{q}\,P_2+(\hat{q}\times\hat{k})\cdot\vec{\varepsilon}P_3\ , \tag{3}$$

with m the proton mass, $s=(p_1+k)^2$ the cms energy squared and ε_μ the photon polarization vector. These four amplitudes (and the additional $L_{0+}, P_{4,5}$ for electroproduction) are calculable within CHPT. Note that we do not expand the prefactor $m/\sqrt{s}$ in what follows. Generically, the chiral expansion of the various multipoles takes the form

$$\mathcal{M}=\mathcal{M}^{\rm Born}+\mathcal{M}^{\rm loop}+\mathcal{M}^{\rm ct}\ , \tag{4}$$

where the Born terms subsume the tree graphs and the anomalous magnetic moment couplings from $\mathcal{L}_{MB}^{(2)}$, 'ct' refers to the remaining counter terms and the loop contribution at order q^3 is given entirely in terms of the parameters from $\mathcal{L}_{M}^{(2)}+\mathcal{L}_{MB}^{(1)}$. These are the Goldstone boson decay constant F_ϕ (we choose here $F_\phi=F_K=113\,\mathrm{MeV}$) and the two axial couplings $F\simeq 0.5$ and $D\simeq 0.75$. The magnetic moments appearing in the Born terms are all well known with the exception of the one for the Σ^0. To determine it, we use the Coleman–Glashow relation (which is exact to the order we are working), $\mu_{\Sigma^0}=[\mu_{\Sigma^+}+\mu_{\Sigma^-}]/2=0.65\,\mathrm{n.m.}$. For the coupling constants, we use the SU(3) predictions $\sqrt{6}g_{p\Lambda K^+}=-(D+3F)g_{\pi N}/(F+D)$ and $\sqrt{2}g_{p\Sigma^0K^+}=(D-F)g_{\pi N}/(F+D)$ with $g_{\pi N}=13.4$ the pion–nucleon coupling constant. Clearly, a more precise knowledge of these coupling constants would be needed to reduce the uncertainty from the Born graphs. For charged kaon photoproduction, one combination of the LECs d_1 and d_2 can be inferred from the nucleon axial radius, $\langle r_A^2\rangle=0.42\,\mathrm{fm}^2$. This constrains the $p\to\Lambda\,K^+$ transition axial radius,

$$|\langle r_A^2\rangle_{p\to\Lambda\,K^+}|=\frac{3\sqrt{2}}{D+3F}(\,d_1+3d_2\,)=0.23\ldots0.70\ \mathrm{fm}^2\ , \tag{5}$$

where the bound is obtained by setting either $d_1=0$ or $d_2=0$ and fixing the non–zero LEC from the proton value. In what follows, we use $\langle r_A^2\rangle_{p\to\Lambda\,K^+}=0.55\,\mathrm{fm}^2$. In the electroproduction case ($k^2<0$), one is also sensitive to kaon and hyperon electromagnetic form factors. For the $K^0\,\Sigma^+$ final state, the neutral kaon form factor to one loop is free of counter terms and rather accurately given [9]. The isovector Dirac radius for the Σ^+ follows to be

$$\langle r_V^2\rangle_{\Sigma^+}=-\frac{(D+F)^2}{8\pi^2F_K^2}\left(5\ln\frac{M_K}{\lambda}-\frac{7}{2}\right)-\frac{D^2+3F^2}{12\pi^2F_\pi^2}\left(5\ln\frac{M_\pi}{\lambda}-\frac{7}{2}\right)+12\,d_{14}+4\,d_{15}\ . \tag{6}$$

Remarkably, the same combination of the LECs $d_{14}+d_{15}$ appears in the isovector proton radius. Taking the value of the most recent dispersion–theoretical calculation for $\langle r_V^2\rangle_p=$

$0.59\,\mathrm{fm}^2$ [10], we predict

$$\langle r_V^2\rangle_{\Sigma^+} = 0.27\ldots 0.33\ \mathrm{fm}^2\ , \tag{7}$$

where the smaller (larger) value refers $F = 0.85\,(0.75)$ and $D = 0.52\,(0.50)$, respectively. We now turn to the loop contributions. In charged kaon production, these lead to complex amplitudes due to the pion rescattering diagram whose threshold is way below the physical production threshold. Consequently, the imaginary parts calculated are significantly too large. This can be understood in terms of the Fermi–Watson theorem. Consider e.g. $\gamma\, p \to K^+\,\Lambda$,

$$\mathrm{Im}\, E_{0+}^{K^+\Lambda} = \mathrm{Re}\, E_{0+}^{\pi^+ n}\cdot\left(-\frac{\sqrt{3}\,M_K}{\sqrt{8}\,F_\phi^2}\right)\cdot\frac{m_\Lambda}{4\pi\sqrt{s}}\cdot\mathrm{PS} \tag{8}$$

making use of the SU(3) generalization of the current algebra prediction for the S–wave πN scattering lengths and PS denotes the pertinent phase space. If one now evaluates the electric dipole amplitude at the $\pi^+ n$ threshold, $E_\gamma = 0.15\,\mathrm{GeV}$, one exactly reproduces the too large result of the one loop calculation to order q^3. To get a more realistic value for these imaginary parts, we take the amplitude $E_{0+}^{\pi^+ n}$ at the energy corresponding to the $K\Lambda$ threshold, $E_\gamma = 0.91\,\mathrm{GeV}$, from the recent compilation of the VPI group [11].[#4] This is similar to what was done in the q^4 calculation of the process $\gamma p \to \pi^0\pi^0 p$ [12]. We remark that these q^3 loop contributions are no longer finite as it is the case in single pion production to this order (calculated in SU(2)). The renormalization procedure to render these divergences finite is standard and discussed in [14].[#5] In what follows, we use $\lambda = 1\,\mathrm{GeV}$, with λ the scale of dimensional regularization. Finally, to estimate the LECs $d_3,\ldots,d_{13}$, we use resonance saturation including the baryon decuplet and the vector meson nonet. A detailed account of this procedure can be found in ref.[14]

4. We now present the results for the various final states (photoproduction case). We use the parameters listed above. A more detailed account of the dependence on these parameters is given in [14].

$\underline{K^0\Sigma^+}$: All LECs are determined by resonance exchange. In Fig.1a, we show the total cross section for the first 100 MeV above threshold. No data point exists in this range so far, but soon the new ELSA data should be available [4]. The electric dipole amplitude is real at threshold, we have $E_{0+}^{\mathrm{thr}}(K^0\Sigma^+) = 1.07\times 10^{-3}/M_\pi$. The coupled channel model based on a tree level chiral Lagrangian at order q^2 gives a larger value $E_{0+}^{\mathrm{thr}}(K^0\Sigma^+) = (1.34 + 3.38i)\times 10^{-3}/M_\pi$ [15]. We remark that in that approach only S–waves are considered and thus the electric dipole amplitude effectively subsumes some of the P–wave contributions treated here. In Fig.1b we show a prediction for the recoil polarization at $E_\gamma = 1.26\,\mathrm{GeV}$ (which is the central energy of the lowest bin of the not yet published ELSA data).

$\underline{K^+\Lambda}$:The total cross section from threshold up to 100 MeV above is shown in Fig.2a. The lowest E_γ bin from ELSA [3] is $0.96 < E_\gamma < 1.01\,\mathrm{GeV}$ and has $\sigma_{\mathrm{tot}} = (1.43\pm 0.14)\,\mu\mathrm{b}$, i.e.

[#4] We neglect the momentum dependence of the P–waves and the corrections to the strong scattering vertex. This needs to be improved.

[#5] Notice that the Feynman graph calculation can be checked against the complete list of divergent operators in SU(3) and their β–functions given in ref.[13].

we slightly underestimate the total cross section. In Fig.2b, we show the predicted recoil polarization P at $E_\gamma = 1.21$ GeV (which is higher in energy than our approach is suited for). Amazingly, the shape and magnitude of the data [3] is well described for forward angles, but comes out on the small side for backward angles. Isobar models [16][17][18], that give a descent description of the total and differential cross sections also at higher energies, fail to explain this angular dependence of the recoil polarization (an exception is the recent work of ref.[19]).
$\underline{K^+\Sigma^0}$:The total cross section is shown in Fig.3a. It agrees with the two data points from ELSA [3]. The recoil polarization at $E_\gamma = 1.26\,\mathrm{GeV}$ is shown in Fig.3b. It has the right shape but comes out too small in magnitude. Nevertheless, we observe the important sign difference to the $K^+\Lambda$ case, which is commonly attributed to the different quark spin structure of the Λ and the Σ^0.[#6] Here, it stems from an intricate interference of the complex S– and P–wave multipoles. In particular, one needs both s– and t–channel resonance excitations to get the shape of P. In any case, one would like to have data closer to threshold and with finer energy binning to really test the CHPT scheme.

5. In summary, we have used three–flavor chiral perturbation theory to investigate threshold kaon production off protons by real (and virtual) photons. Fixing all unknown parameters from single baryon properties and making use of the resonance saturation hypothesis, we achieve a satisfactory description of the few threshold data. In particular, the shape of the angular dependences of the Λ and Σ^0 polarization at $E_\gamma \simeq 1.2\,\mathrm{GeV}$ is similar to the empirical ones. Clearly, these results should only be considered indicative since we have to include (a) higher order effects (for both the S– and P–waves), (b) higher partial waves and (c) have to get a better handle on the ranges of the various coupling constants. In addition, one would also need more data closer to threshold, i.e. in a region where the method is applicable. However, the results presented are encouraging enough to pursue a more detailed study of these reactions (for real and virtual photons) in the framework of chiral perturbation theory.

References

[1] V. Bernard, N. Kaiser and Ulf-G. Meißner, Z. Phys. C70 (1996) 483

[2] V. Bernard, N. Kaiser and Ulf-G. Meißner, Phys. Lett. B378 (1996) 337

[3] M. Bockhorst et al., Z. Phys. C63 (1994) 37

[4] W. Schwille, private communication

[5] E. Jenkins and A.V. Manohar, Phys. Lett. B255 (1991) 558

[#6] Notice that this argument is strictly correct for massless quarks only.

[6] V. Bernard, N. Kaiser, J. Kambor and Ulf-G. Meißner, Nucl. Phys. B388 (1992) 315

[7] G. Ecker et al., Nucl. Phys. B321 (1989) 311

[8] V. Bernard, N. Kaiser and Ulf-G. Meißner, Z. Phys. C60 (1993) 111

[9] J. Gasser and H. Leutwyler, Nucl. Phys. B250 (1985) 465

[10] P. Mergell, Ulf-G. Meißner and D. Drechsel, Nucl. Phys. A596 (1996) 367

[11] R. A. Arndt, I. I. Strakovsky and R. L. Workman, Phys. Rev. C53 (1996) 430

[12] V. Bernard, N. Kaiser and Ulf-G. Meißner, Phys. Lett. B382 (1996) 19

[13] G. Müller and Ulf-G. Meißner, preprint KFA-IKP(Th)-1996-07 and TK 96 24

[14] S. Steininger, Diploma thesis, University of Bonn, 1996;
S. Steininger and Ulf-G. Meißner, in preparation

[15] N. Kaiser, T. Waas and W. Weise, preprint TUM/T39-96-20, Nucl. Phys. A, in print

[16] R.A. Adelseck and B. Saghai, Phys. Rev. C42 (1990) 108; C45 (1992) 2030

[17] R. Williams, C. Ji and S. Cotanch, Phys. Rev. C46 (1992) 1617

[18] T. Mart, C. Bennhold and C.E. Hyde-Wright, Phys. Rev. C51 (1995) R1074

[19] B. Saghai and F. Tabakin, preprint DAPNIA-SPhN-96-18, to app. in Phys. Rev. C

[20] R. Erbe et al., Phys. Rev. 188 (1969) 2060

Figure Captions

Fig. 1 (a) Total cross section for $\gamma p \to K^0\Sigma^+$ (solid line). The S–wave contribution is given by the dotted line. (b) Recoil polarization at $E_\gamma = 1.26\,\mathrm{GeV}$.

Fig. 2 (a) Total cross section for $\gamma p \to K^+\Lambda$ (solid line). The S–wave contribution is given by the dotted line. (b) Recoil polarization at $E_\gamma = 1.21\,\mathrm{GeV}$. The data are from ref.[3]. The two data points from ref.[20] in this interval are not shown.

Fig. 2 (a) Total cross section for $\gamma p \to K^+\Lambda$ (solid line). The S–wave contribution is given by the dotted line. (b) Recoil polarization at $E_\gamma = 1.26\,\mathrm{GeV}$. The data are from ref.[3].

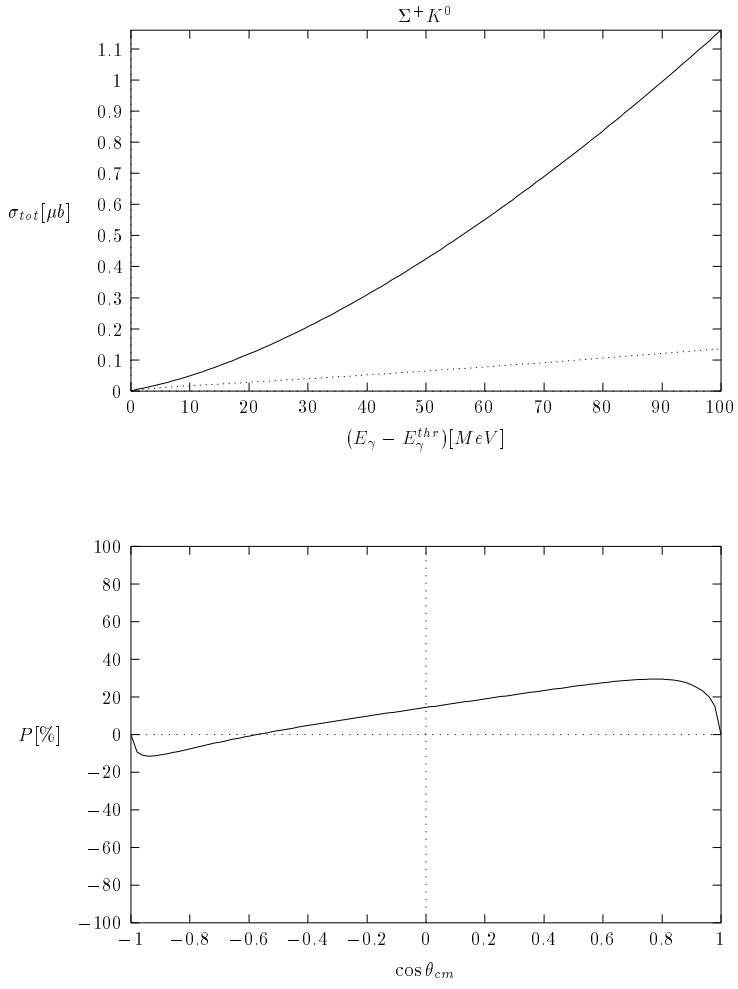

Figure 1

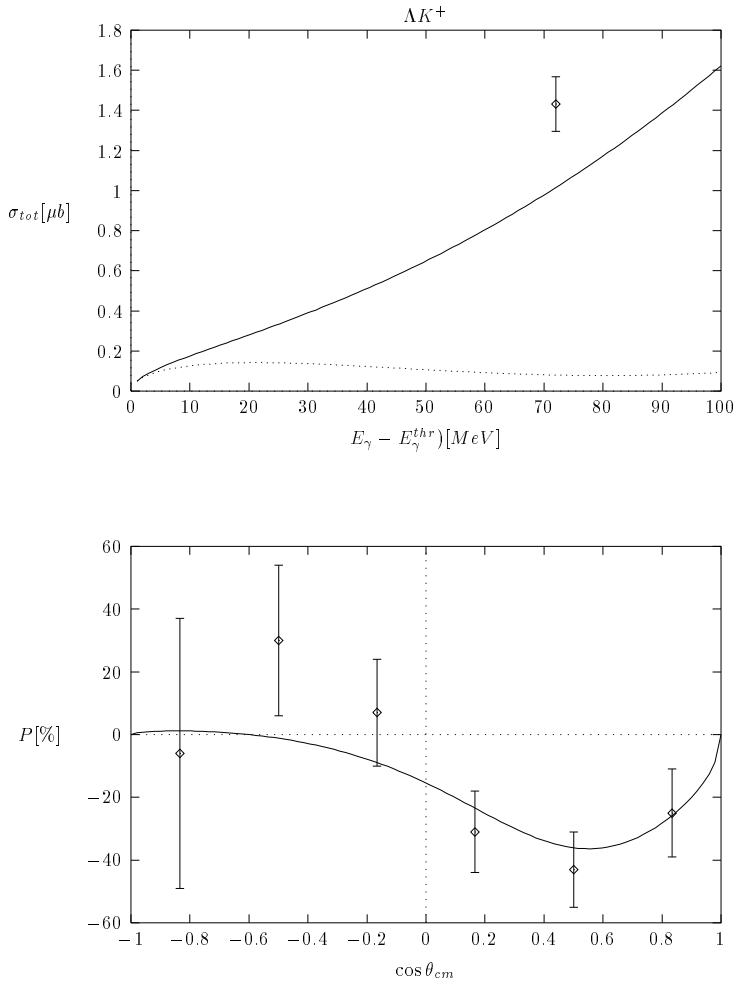

Figure 2

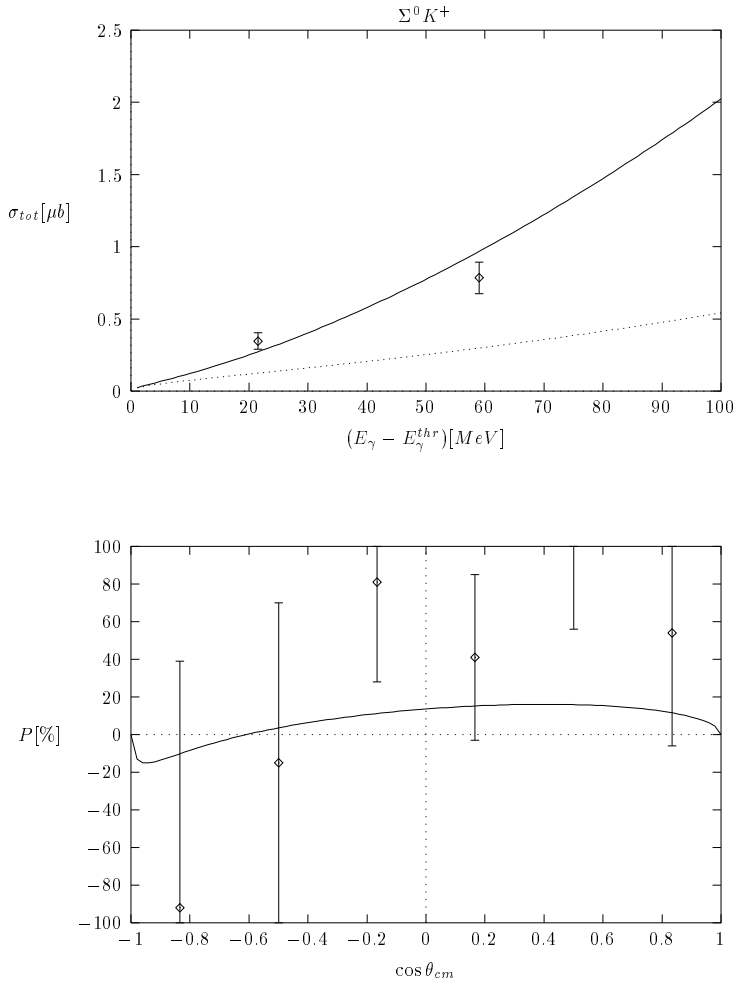

Figure 3